Comparison of T1 Mapping by Cardiac MRI to Non-cardiac MRI Methods to Evaluate Cardiac Fibrosis

4

Róisín B. Morgan, Michael Jerosch-Herold, and Raymond Y. Kwong

Introduction

Myocardial fibrosis is a pathological process involving extracellular matrix (ECM) remodeling.

In practical terms, the two basic types of fibrosis are focal and diffuse. Focal fibrosis is defined as scar (e.g., myocardial infarction) or focal patches of scar interspersed within the normal myocardium, as is the case in many cardiomyopathies. Conversely, the presence of diffuse, reactive fibrosis is increasingly recognized in a variety of conditions, even in the absence of myocardial ischemia. The structure and composition of the myocardial extracellular matrix (ECM) ensure the harmonic structure and function of the heart and mediate cell to cell and cell to ECM molecular signaling and interactions [1]. In myocardial disease, increased ECM deposition is a crucial compensatory and repair process. Replacement fibrosis, a process that typically occurs after the loss of cardiomyocytes post–myocardial infarction (MI), contributes to maintaining the macroanatomy of the heart. On the other hand, reactive fibrosis occurs in response to cardiac stress and is seen in most cardiac diseases with pressure [2] and volume overload [3], underlying cardiomyopathy such as HCM [4], ARVC [5] or DCM [6], and in areas of post-MI remodeling in the noninfarcted area [7].

Regardless of the etiology, fibrosis causes increased myocardial stiffness thus promoting cardiac dysfunction. Clinically, these patients present with symptoms of cardiac failure although in many cases this is a subclinical disease and may present at a later stage. As discussed in this chapter, imaging techniques such as echocardiography, cardiac magnetic resonance (CMR), multidetector cardiac computed tomography (MDCT) and nuclear imaging have been proven to detect early features of systolic and diastolic left ventricular (LV) dysfunction and impaired contractile reserve. The evolving field of CMR and molecular techniques may shortly lead to the further identification of diffuse reactive fibrosis. The goal of such new modalities is to promote and enable targeted therapy to be instituted earlier, thus, leading to prevention of disease progression and fibrosis accumulation long term.

Traditionally, endomyocardial biopsy has been the method utilized for quantification of myocardial interstitial collagen content. However, imaging techniques and serum collagen biomarkers may be used as surrogate markers of

R. B. Morgan · R. Y. Kwong (✉)
Non-invasive Cardiovascular Imaging, Cardiovascular Division, Department of Medicine, Brigham and Women's Hospital, Harvard Medical School, Boston, MA, USA
e-mail: rmorgan@mmc.org; rykwong@partners.org

M. Jerosch-Herold
Department of Radiology, Brigham and Women's Hospital, Harvard Medical School, Boston, MA, USA
e-mail: mjerosch-herold@bwh.harvard.edu

myocardial fibrosis [8]. These imaging methods may be divided into methods to visualize fibrosis (CMR, MDCT, and nuclear imaging) and techniques to assess subtle subclinical LV systolic and diastolic dysfunction (predominantly echocardiographic). These methods are discussed in detail below.

Cardiac MRI (CMR)

In CMR imaging, the signal intensity of the pixel is based on the relaxation of hydrogen nuclei protons in the static magnetic field, the strength of which is measured in Tesla (T), and typically 1.5 or 3.0T for cardiac imaging. The relaxation of the hydrogen nucleus proton is characterized by two very distinct MR relaxation parameters. First, the T1 or spin-lattice relaxation time corresponds to a specific time constant when the 1H nuclear magnetization has recovered to roughly 63% of its equilibrium value after magnetization inversion. Secondly, the transverse relaxation time (T2) or spin-spin relaxation time corresponds to the specific time when the 1H transverse magnetization created by a radio-frequency (RF) pulse excitation drops to roughly 37% of its initial value right after the RF pulse [9]. Both of these time constants depend on the molecular environment of the water molecules in the tissue and thus they characterize each tissue specifically. Times vary significantly from one type of tissue to another, but also can vary within the same tissue depending on its pathophysiological status (e.g. inflammation, edema, fibrosis).

Late gadolinium enhancement cardiac MRI (LGE-CMR) has become the clinical reference standard for determining the presence and extent of myocardial infarction in ischemic heart disease. For nonischemic cardiomyopathy, it has become an effective tool providing an accurate, non-invasive detection of focal myocardial fibrosis with both diagnostic and prognosis values. It has been extensively validated against histopathological examination in nonischemic conditions [10, 11] and ischemic heart disease [12]. After injection of intravenous gadolinium contrast (Gd), distinct enhancement patterns occur in different myocardial disorders, all characterized by tissue disarray, fibrosis, and inflammation [13–17]. Regardless of the etiology, myocyte injury typically leads to increased myocardial collagen content and a marked reduction of cardiomyocyte volume [18]. Gd-based contrast agents permeate the extra-cellular space, leading to enhancement in regions of focal myocardial necrosis. The physiological basis of the LGE of myocardial fibrosis is based on the combination of an increased volume of distribution for the contrast agent and a prolonged wash-out related to the decreased capillary density within the myocardial fibrotic tissue [12, 19]. In CMR, the discrimination between scarred/fibrotic myocardium and normal myocardium relies on contrast concentration differences in addition to the chosen setting of the inversion-recovery sequence parameters (TI-time). These parameters are set to "null" the normal myocardial signal that appears dark in the final image relative to the bright signal of the scarred/fibrotic myocardium as shown in Fig. 4.1 [9].

Although LGE-CMR allows a very sensitive and reproducible qualitative assessment of myocardial replacement fibrosis, it is limited to cases where focal necrosis produces a localized loss of cardiomyocytes, that can be contrasted against other regions in the heart that remain viable. A diffuse loss of cardiomyocytes and concurrent expansion of the extra-cellular matrix can be difficult to visualize and quantify with LGE imaging, as it resembles more of a binary diagnostic test, rather than a method that can detect the build-up of fibrosis as a continuum. As a result, in recent years T1 and T2 mapping techniques have been developed by the CMR community to quantify myocardial fibrosis accurately. Recent technical improvements in acquisition sequences have enabled us to perform myocardial T1mapping with high spatial resolution by using both 1.5 and 3T magnetic resonance imaging scanners within a single breath hold [20, 21]. Compared with LGE imaging, T1 mapping by CMR before and after contrast administration provides a continuous measure of extra-cellular volume (ECV) expansion that correlates in my cardiac conditions closely with the build-up of
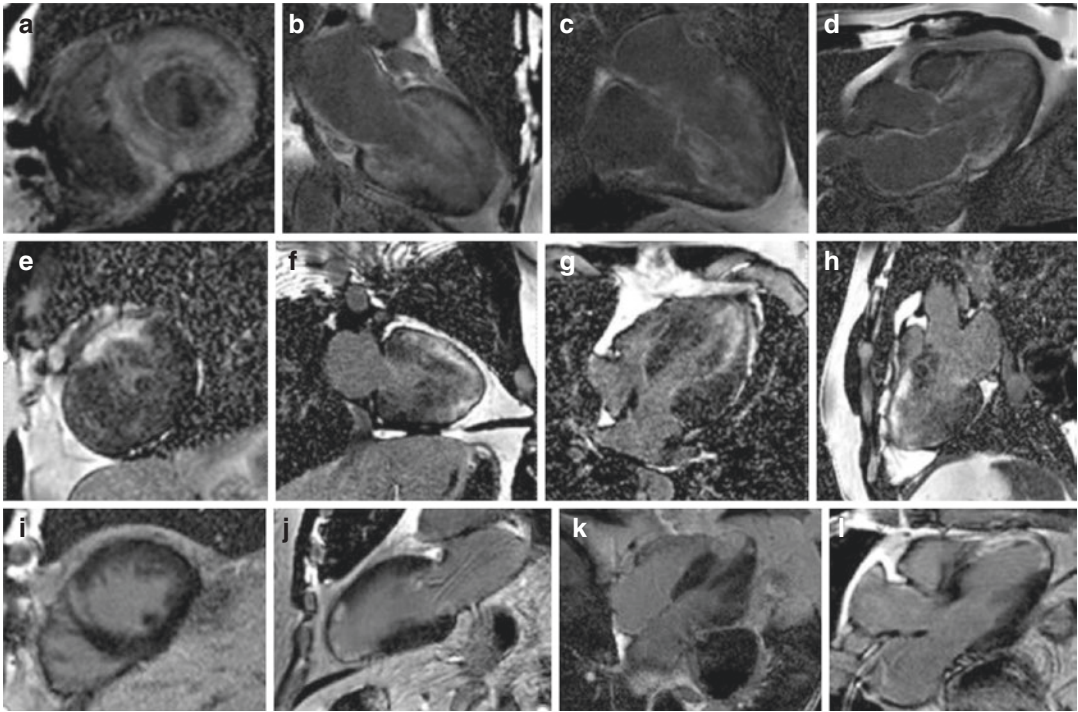
Fig. 4.1 LGE-CMR images from patients with myocardial fibrosis caused by cardiac amyloidosis (**a–d**), hypertrophic cardiomyopathy (**e–h**) and ischemic cardiomyopathy with evidence of prior subendocardial infarction in the distribution of the distal LAD (**i–l**). Gadolinium contrast media accumulates in the abnormal fibrotic myocardium and appears bright in contrast to the normal myocardium (dark). The distribution and extent of LGE in these examples are classic for the associated condition

interstitial fibrosis. It thus allows quantification of ECV on a standardized scale of each myocardial voxel to characterize myocardial tissue [9]. The myocardial native T1 (i.e. measured without giving any contrast agent) can by itself also provide an indication of tissue pathology, but in the case of diffuse fibrosis the origin of changes in native T1 can encompass a range of conditions such as edema, and also the build of connective tissue.

In practice, by reconstructing a sequence of images corresponding to various times after an magnetization inversion (TI), T1 maps can be generated in which each pixel intensity value represents the T1 relaxation time (e.g., in ms). A key requirement is that all images are acquired in the same of the cardiac cycle, so that the inversion recovery can be tracked for single pixels. For this purpose, Messroghli et al. [20] introduced the Modified Look-Locker Inversion-recovery

(MOLLI) sequence, which has become a standard in CMR T1 mapping. More recently, a short MOLLI (modified Look-Locker inversion recovery) sequence has been described, which approximately halved the required breath hold duration and the number of required heartbeats decreased from 17 to 9 [21], but requires more complex processing to generate T1 maps. From a clinical perspective, shMOLLI has enabled significant reduction of the duration of the scan and the quality of the T1 maps is arguably improved due to shorter breath hold time and reduced residual motion.

Areas of diffuse myocardial fibrosis have greater T1 values than normal tissue before intravenous Gd-based contrast media (Gd) is given. Post-Gd administration, T1 value is lower than normal in diffuse myocardial fibrosis. The reason for this lies in the fact that the expanded extracellular space in diffuse fibrosis accumulates more

Gd-based contrast than the healthy tissue with compact myocytes. A reduction in T1 value is not specific for diffuse myocardial fibrosis; however, T1 reduction may also occur with cardiomyopathies where the extracellular space is expanded such as in amyloid depositions [22].

A number of validation studies have been carried out comparing histology to T1 mapping and ECV values. That being said, Iles et al. [23] examined a symptomatic heterogeneous heart failure population using post-contrast MOLLI. They compared post-transplant myocardial biopsies with T1 values and demonstrated an inverse correlation between T1 values with percentage fibrosis. They also found a reduction in T1 with worsening diastolic function. Sibley et al. used a post-contrast Look-Locker technique and also demonstrated an inverse correlation between T1 time and histological fibrosis on myocardial biopsy in patients with a broad range of cardiomyopathies [24]. Studies that are based on the use of post-contrast T1, rather than derivation of ECV, for the detection of diffuse fibrosis, require careful standardization of the time between contrast-injection and T1 mapping, to eliminate the potential confounding variable of contrast clearance times. Furthermore, the post-contrast T1 will also depend on the rate of renal clearance of the contrast agent, introducing the patients' renal function as additional confounder. ECV, which is calculated as the change of the myocardial T1 rate constants (inverse of the measured myocardial T1) between pre- and post-contrast states, normalized by the change of the blood T1 rate constants (inverse of the measured blood T1), is largely independent of the rate of contrast clearance. Also, ECV values are also independent of scanner field strength since this measurement is a ratio of the changes in myocardial-blood rate constants, which is in contrast to T1 values that increase with field strength both for native- and post-contrast T1 measurements. Robustness of ECV derivation is also enhanced by capturing the myocardial and blood wash-in and wash-out dynamics during the 15–30 min period after Gd injection by acquiring multiple post-contrast T1 map in addition to the pre-contrast T1 map. Table 4.1 explores the various studies to date, investigating the use of T1 map in various cardiac conditions associated with myocardial fibrosis.

In practice, myocardial T1 mapping is technically demanding and standardization of the methodology is required. The CMR community has made a concerted effort at standardization [37]; however, in the coming years, the routine use of T1 map for clinical evaluation of myocardial fibrosis will become more user-friendly and less time-consuming for routine clinical practice.

Novel CMR Approaches

Concerns about the administration of Gd-bound contrast agents (GBCA) to patients with poor renal function have provided a strong impetus for developing CMR methods that do not rely on GBCA for the detection of diffuse fibrosis. With the standard imaging techniques, generally the signal from 1H nuclei in connective tissue components such as collagen is not detected due to the very short T2 constants for collagen 1H nuclei that are approximately 1 ms. Standard T1-mapping techniques such as MOLLI [38] do not detect or detect poorly the signal components from 1H nuclei in connective tissue. A direct detection of the 1H signal from connective tissue components such as collagen can be achieved with imaging sequences that use ultra-short echo times (UTE) on the order of a fraction of a millisecond. UTE imaging is increasingly seen as a promising approach for the detection of diffuse fibrosis by measuring the fraction of 1H signal that comes from connective tissue relative to the 1H signal from mobile 1H nuclei. Initial studies have demonstrated encouraging feasibility of this approach for detecting diffuse fibrosis [39]. The 1H signal from collagen is shifted relatively to the 1H from the mobile 1H nuclei by −3.2 ppm. The decay of the 1H signal from myocardial tissue as a function of the echo-time, therefore, can be described as a bi-exponential decay where the relatively quick decaying collagen component oscillates as a function of the 3.2 ppm 1H frequency shift for the collagen component. Using this type of model for the myocardial signal

Table 4.1 Data supporting the use of T1 mapping in the evaluation of myocardial fibrosis and the conditions studied

Author and date	Disease	Technique	Conclusion
Messroghli [25] 2003	Acute Myocardial Infarction	Look-Locker	In acute MI patients post-contrast T1 values were significantly lower than normal myocardium T1 values
Maceira [26] 2005	Amyloidosis	Look locker	Subepicardial post-contrast T1 values were significantly reduced in cardiac amyloidosis patients compared with controls
Messroghli [27] 2007	Myocardial infarction, acute or chronic	MOLLI	In acute and chronic myocardial infarction, pre-contrast T1 values were higher than T1 values in remote myocardium
Iles [23] 2008	Heart failure	VAST	Post-contrast myocardial T1 times correlated histologically with fibrosis and were shorter in heart failure subjects than controls (p 0.0001) [23]. The post-contrast myocardial T1 time reduced as diastolic function worsened
Broberg [28] 2010	Adult congenital heart disease	Look-Locker	Patients with ACHD have diffuse, extracellular matrix remodeling similar to patients with acquired heart failure as measured by T1 mapping
Flett [29] 2010	Aortic stenosis. HCM	Look-Locker	A high correlation was seen between T1 mapping with equilibrium contrast CMR and histologic fibrosis in aortic stenosis and HCM
Gai [30] 2011	Diabetes mellitus	Look-Locker	A significant difference was noted in post-contrast T1 values between those at low risk of diabetes compared with those at high risk
Bauner [31] 2012	Chronic MI	MOLLI	A significant difference was noted in post-contrast T1 values in chronic myocardial infarct regions compared to healthy myocardium
Turkbey [32] 2012	Myotonic Dystrophy	Look locker	Postcontrast myocardial T1 time was shorter in myotonic dystrophy patients compared to controls, likely reflecting the presence of diffuse myocardial fibrosis
Dass [33] 2012	HCM/DCM	ShMOLLI	HCM/DCM patients had higher pre-contrast T1 times than controls
Fontana [34] 2012	HCM, AS, amyloid	ShMOLLI	ECV quantification using single breath-hold ShMOLLI T1 mapping can measure ECV by EQ-CMR across a spectrum of interstitial expansion
Rao [35] 2013	Diabetes	Look locker	The myocardial ECV in this diabetic population was elevated compared with published values of ECV in healthy subjects and with the mean ECV of 0.27 ± 0.03 ($p < 0.0001$) obtained in healthy, normotensive volunteers
Ellims [36] 2014	Post-cardiac transplant	VAST	Diffuse myocardial fibrosis (as assessed by post-contrast myocardial T1 time), correlates with invasively-demonstrated LV stiffness in cardiac transplant patients
Ntusi 2015	Rheumatoid Arthritis	ShMOLLI	Focal fibrosis (LGE) was found in 46% of RA patients compared with none of the controls. Larger areas of focal myocardial edema were seen in patients with RA. They also had higher native T1 values, larger areas of involvement as indicated by native T1 > 990 ms and expansion of ECV compared with controls

decay as a function of TE, one can show that the collagen signal fraction changes linearly with collagen concentration [40], suggesting feasibility in fibrosis quantitation.

Another approach with the same goal of quantifying the connective tissue fraction in the myocardium is based on a technique termed chemical-exchange saturation transfer (CEST) imaging. The endogenous CEST between macromolecules in fibrotic scar tissue and surrounding water has been investigated in a murine model of myocardial infarction (MI). CEST contrast is generated through frequency-selective RF saturation to exchange the magnetization between scar tissue and surrounding water in normal myocardium, followed by image-acquisition. The signal read-out

during the image-acquisition is thereby encoded by the molecular signature of the target tissue of interest (e.g. fibrotic tissue). A recent study [41] has shown the feasibility of detecting scar tissue though it remains uncertain whether the diffuse interstitial fibrosis, a more challenging target than infarct scar, can be quantified with this technique.

Another approach aimed at the direct detection of scar and fibrosis is based on the use of targeted contrast agents, specifically the use of collagen-binding contrast agents. In this type of contrast agents, the wash-out time constants in regions of post-infarction scar become significantly longer, compared to a Gd-based contrast agent without binding affinity for collagen or other myocardial scar components [42]. To-date it remains unclear if such collagen-binding contrast agents are also suitable for the detection of diffuse interstitial fibrosis. The approach for detecting diffuse interstitial fibrosis with a collagen-binding contrast agent is likely to involve T1-mapping to quantify collagen-bound fraction of contrast.

Nuclear Imaging

Molecular imaging techniques for detecting diffuse myocardial fibrosis using SPECT or PET imaging are predominantly research-based tools with great potential for future clinical use [1, 7, 43]. Ischemic fibrosis, however, may be readily detected, using myocardial perfusion techniques, which are currently in routine clinical practice.

Radionuclide imaging techniques are frequently used in the evaluation of patients with known or suspected CAD. These techniques use radiolabeled drugs or radiopharmaceuticals which are injected intravenously and trapped in myocardial tissue. Radioactivity within the heart decays by emitting gamma rays. The interaction between these gamma rays and the detectors in specialized scanners—single photon emission computed tomography (SPECT) and positron emission tomography (PET)—creates a scintillation event, which can be captured by digital recording equipment to create an image of the heart. Electrocardiogram (ECG)-triggered gated rest and stress images are acquired after intravenous injection of the radiopharmaceutical and used to define the extent and severity of myocardial ischemia and scar as well as regional and global cardiac function and remodeling. In SPECT imaging, technetium-99m (99mTc)-labeled tracers are frequently used because they generate the best image quality and the lowest radiation dose to the patient. After intravenous injection, these tracers become trapped intracellularly in mitochondria and show minimal change over time (Figs. 4.2 and 4.3).

PET myocardial perfusion imaging (MPI) is an alternative to SPECT and is associated with improved diagnostic accuracy and lower radiation dose to the patient. To evaluate myocardial viability in post-MI patients, myocardial perfusion imaging with SPECT or PET usually is combined with metabolic imaging—specifically, 18F-fluorodeoxyglucose (FDG) PET. The presence of a reversible myocardial perfusion defect is indicative of ischemia whereas a fixed perfusion defect generally reflects scarred myocardium (area of fibrosis) from previous infarction. 18F-FDG is used to assess regional myocardial glucose utilization and compared to perfusion
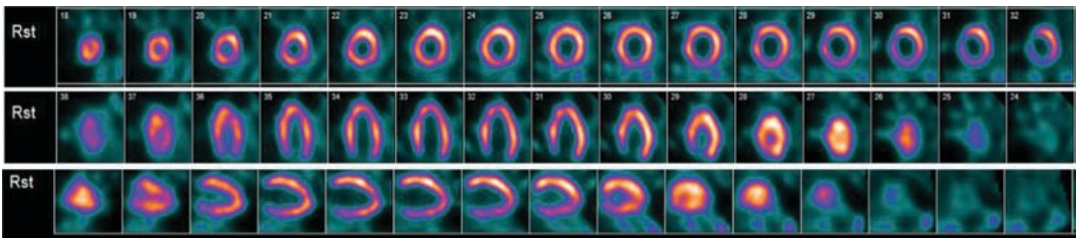
Fig. 4.2 Rest myocardial perfusion images in a normal patient with normal myocardial uptake of sestamibi seen in short axis, vertical long axis and horizontal long axis images (top, middle and bottom rows respectively)
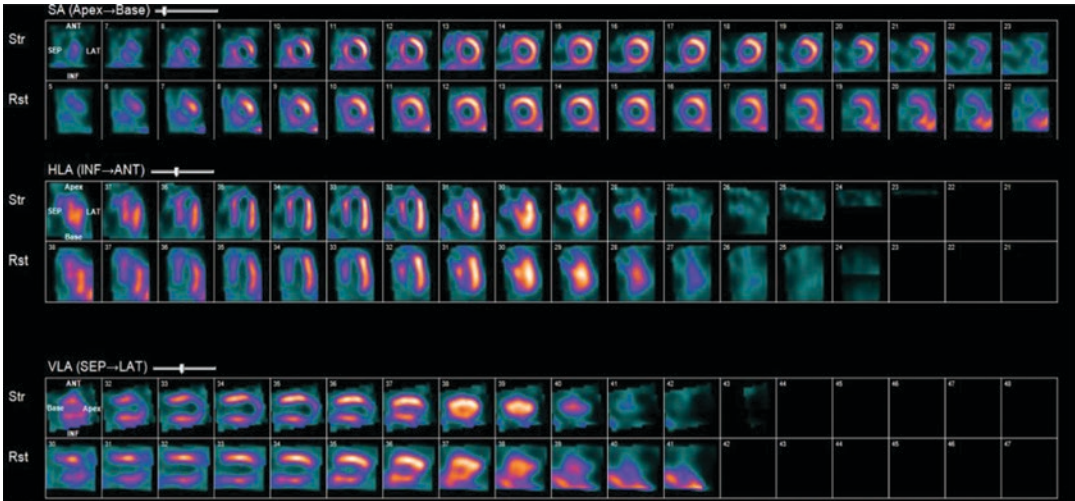
Fig. 4.3 Stress (top row) and rest perfusion (bottom row) images in a patient with a medium to large region of myocardial fibrosis (scar) in the distribution of the mid left anterior descending (LAD) artery, with minimal ischemia

images to define metabolic abnormalities associated with infarction and hibernation. Myocardial regions showing reduced perfusion and increased FDG uptake at rest (so-called *perfusion-FDG mismatch*) identify areas of viable but hibernating myocardium, whereas regions showing reduced perfusion and FDG uptake at rest (so-called *perfusion-FDG match*) are consistent with myocardial scar or fibrosis.

Using $H2^{15}O$ and $C^{15}O$ tracers, PET can assess the perfusable tissue index (PTI), i.e. the fraction of the myocardium that is perfusable by water [44]. As fibrotic myocardium is unable to exchange water rapidly, a reduction in this variable may correlate with fibrosis. PTI, reduced in patients with advanced dilated cardiomyopathy [45], correlates with reduced contractile function [46] and is also present in areas of focal fibrosis following MI [47]. However, its use has not been validated in a histological comparison study. Technetium-99m-labelled Cy5.5-RGD injection followed by PET imaging [48] has been shown in animal models as a tracer that binds to myofibroblast cells and correlates with new collagen deposition in an experimental model of myocardial infarction [7]. These techniques are not in routine clinical use, and although they have shown promising results, currently they are not applicable to patients in the current era.

Hypertrophic cardiomyopathy patients may show abnormalities and replacement fibrosis on myocardial SPECT and positron emission tomography (PET) indicative of underlying abnormalities of oxidative metabolism, which may precede myocardial perfusion abnormalities and replacement fibrosis [49]. Impaired metabolism has been noted in up to 73% of segments when radiotracers such as FDG, C-acetate or 123I-BIMPP were used; these observations suggest that the impairment of long-chain fatty acid metabolism may precede other metabolic abnormalities in HCM patients [50]. Another study examining myocardial fibrosis in HCM patients who underwent LGE-CMR, Tc99m-MIBI SPECT, and I23-BIMPP SPECT [51] showed that segments with a larger extent of replacement fibrosis on LGE-CMR had more abnormalities in perfusion and metabolism on SPECT.

Echocardiography

Backscatter

The reflectivity of tissue to ultrasound is a noninvasive measure of myocardial tissue characterization and collagen deposition that has been used for multiple decades [52]. Qualitative M-mode and 2D echo imaging techniques have

been widely used for scar detection and wall motion assessment in ischemic fibrosis. In addition to these methods, backscatter techniques were developed in the 1980s to quantify myocardial tissue changes characteristic of fibrosis in conditions such as HCM and hypertension [53]. This quantitative echocardiographic estimation of fibrosis was predominantly performed via ultrasonic video densitometric and texture analysis [43]. The relationship between backscatter and histologically quantitated collagen has been confirmed in the literature [54]. Noninvasively, amplitudes of integrated backscatter have also been correlated with elevated pro-collagen concentration [55].

Two myocardial backscatter parameters have been established for use: (1) magnitude of cyclic variation in integrated backscatter, which is a marker of regional function, and although abnormal in conditions of diffuse fibrosis, this parameter has been largely replaced by myocardial strain, and (2) calibrated integrated backscatter. A greater calibrated integrated backscatter is indicative of larger fibrosis [43]. This technique has been used to establish a transmural trend of fibrosis in non-transmural infarction and hence could potentially be employed to assess fibrotic gradients in conditions, such as diabetic heart disease or Duchenne muscular dystrophy with predominantly endocardial or epicardial fibrosis, respectively [56, 57]. Elevated backscatter also occurs with systemic sclerosis although predominantly in the diffuse rather than the limited subgroup [58].

Tissue Doppler Imaging (TDI)

Doppler echocardiography relies on the detection of the shift in frequency of ultrasound signals reflected from moving objects. Conventional Doppler techniques evaluate the velocity of blood flow by measuring high frequency, low amplitude signals from small, fast-moving blood cells [59]. In Tissue Doppler imaging (TDI), these principals are used to quantify the high amplitude, low-velocity signals of myocardial tissue motion. This in turn serves as a measure of myocardial function, typically reduced in the fibrotic heart.

Pulsed wave TDI is used to measure peak myocardial velocities and performs well at the measurement of long-axis ventricular motion, mostly because the longitudinally oriented endocardial fibers are most parallel to the ultrasound beam in apical views of the heart.

Reduction of longitudinal function appears to be one of the most sensitive markers of subclinical heart disease in many conditions associated with fibrosis, including diabetes and hypertension [43]. The impairment of longitudinal function reflects the principal initial involvement of subendocardial fibers, followed by compensation by mid-wall fibers and subsequent improvement in radial contractility to maintain overall cardiac function [57].

Because the apex remains relatively stationary throughout the cardiac cycle, mitral annular motion is a good surrogate marker of overall longitudinal left ventricular contraction and relaxation [60]. Systolic myocardial velocity (Sa), measured at the lateral mitral annulus is a measure of longitudinal systolic function and has been correlated with measurements of LV ejection fraction (EF) [61]. When carrying out an assessment of left ventricular diastolic function, transmitral velocities are directly related to left atrial pressure (preload) and independently related and inversely related to ventricular relaxation [59]. Because of intrinsic differences in myocardial fiber orientation, septal Ea velocities are slightly lower than lateral Ea velocities.

In adults over 30 years old, a lateral Ea velocity >12 cm/s is associated with normal LV diastolic function [62] (Fig. 4.4a). Reductions in lateral Ea velocity to ≤8 cm/s in middle-aged to older adults indicate impaired LV relaxation. In cases of restrictive cardiomyopathy, the characteristic intrinsic myocardial abnormalities result in impaired relaxation and reduced Ea velocities.

Peak systolic and early diastolic myocardial tissue velocities have been used to identify early subclinical disease despite normal conventional echocardiographic values in several progressive, nonischemic fibrotic processes [43]. A reduction in both parameters has been detected in patients with diabetes but no evidence of heart failure,
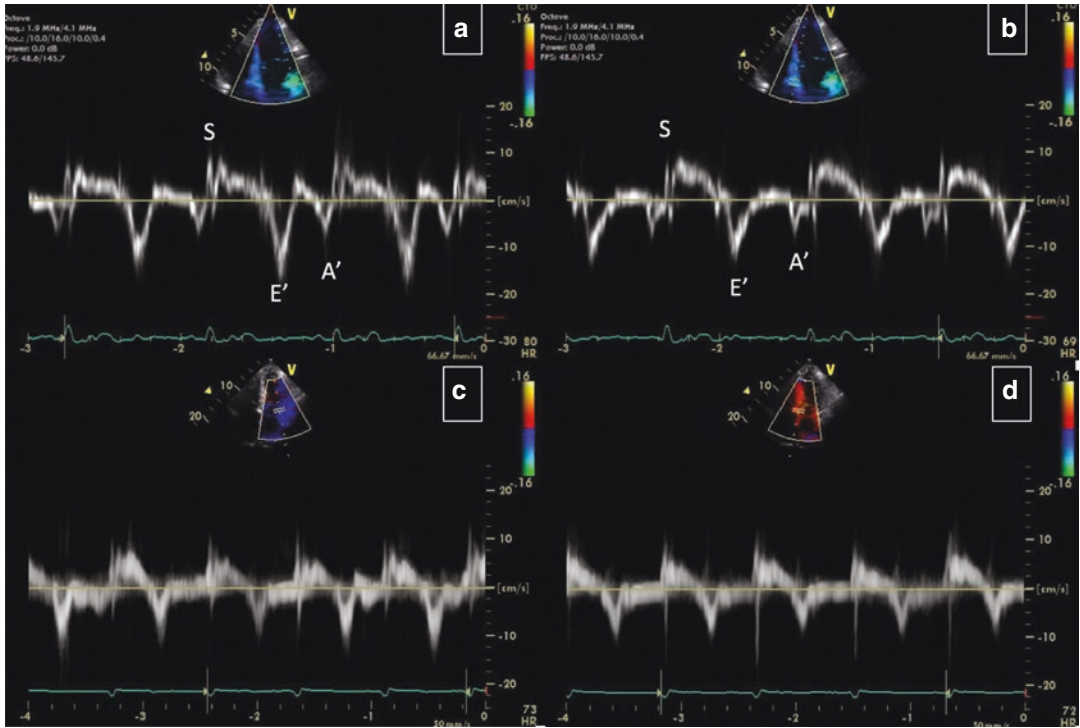
Fig. 4.4 TDI of the lateral (**a**) and septal (**b**) mitral annulus in a normal subject. There are three major velocities: systolic velocity, S′ or Sa, which reflects the systolic function of the left ventricle; E′ or Ea which reflects the status of myocardial relaxation (Normal E′ medial is 10 cm/s

and lateral is >15 cm/s); and A′ or Aa is also related to diastolic function of the left ventricle. Panels (**c** and **d**) are from a patient with cardiac amyloidosis and show fusion of the E′ and A′ waves due to underlying atrial fibrillation

and early diastolic tissue velocity has also been found to be reduced with advancing age and hypertension [63]. This impairment in myocardial velocity and resultant impaired ventricular relaxation may reflect interstitial fibrosis, altered cardiomyocyte cytoskeleton properties, or a combination of both. This relationship is supported by endomyocardial biopsy findings that inversely relate percent fibrosis to tissue Doppler-derived systolic and early diastolic tissue velocity [64].

In a recent study of echo versus cardiac MRI post aortic valve replacement (AVR) in patients with severe AS, LGE+ patients had lower E′, S′, and had higher E/E′ [65]. These findings indicate that echo may be used clinically in patients with contraindication to CMR. TDI E′, especially, is a clinically useful clue of risk stratification before AVR in patients with severe AS and preserved LV systolic function. Another study comparing TDI with CMR-LGE imaging showed that subjects

with normal diastolic function by TDI exhibited no or minimal fibrosis (median LGE score 0, IQR 0–0) [66]. In contrast, the majority of patients with cardiomyopathy (regardless of etiology) had abnormal diastolic function indices by Doppler echo, and substantial fibrosis (median LGE score 3, IQR 0–6.25). In this study, the prevalence of LGE-positivity by diastolic filling pattern was 13% in normal patients, 48% in impaired relaxation, 78% in pseudo-normal and 87% in restrictive filling pattern (p < 0.0001) [54].

Strain and Strain Rate Imaging
Myocardial velocities measured with TDI can be overestimated by translational motion of the myocardium or underestimated by myocardial tethering. As a result, it is useful to measure the actual extent of myocardial deformation by strain and strain rate imaging. Strain is defined as the change in length of a segment of myocardium

relative to its resting length and is expressed as a percentage; strain rate is the rate of this deformation [67]. By convention, shortening is represented by negative values and lengthening by positive values for both strain and strain rate [68]. In a normal individual, longitudinal strain rate values are similar from base to apex. It is possible using a curved cursor during image acquisition, to measure regional strain rate. Ultimately the ultrasound beam needs to be aligned parallel with the direction of myocardial motion. By measuring regional myocardial function, TDI and strain imaging have potential incremental value for the evaluation of cardiomyopathy and diastolic heart failure. Thick myocardial walls due to infiltration or primary cardiomyopathy have reduced TDI and strain values. This is in contrast to normal values obtained in an athlete's heart. It is also useful how the pattern of regional dysfunction can help to identify various underlying cardiomyopathies [69, 70]. In general, global strain measures typically perform better than LVEF in predicting risk [71], and at least two studies suggest that they also offer incremental value beyond clinical information and LVEF [72, 73].

Speckle Tracking Echo
This method quantifies myocardial motion in various planes using 2D images. Reflection, scattering and interference of the ultrasound beam in the myocardial tissue produce a speckle formation [68]. Myocardial regions have unique speckle patterns, which can be tracked from frame to frame throughout the cardiac cycle [69]. Thus an assessment can be made of LV rotational motion, typically referred to as torsion or twist. LV myocardial fibers have a spiral shape, which results in a complex three-dimensional torsion mechanism for systolic contraction and untwisting for diastolic relaxation [74]. The LV subendocardial layer wraps around the LV cavity in the direction of a right-handed helix. In contrast, the subepicardial layer wraps around in the direction of a left-handed helix. When viewed from the LV apex, apical rotation is counterclockwise, and basal rotation is clockwise during systole [68]. Speckle tracking can be used for quantification of LV systolic and potentially diastolic function. In

addition, it can be used for measuring strain instead of TDI as discussed above.

Recent work aiming to explore whether LV twist analysis can detect the extent of myocardial fibrosis in patients with hypertrophic cardiomyopathy (HCM) showed that HCM patients had significantly higher basal (Bas)-Rotation, anteroposterior (AP)-Rotation, LV Twist, left ventricular ejection fraction (LVEF), left atrium end systolic dimension (LADs), interventricular septal thickness (IVST), left atrial volume index (LAVi), E/Em and left ventricular mass index (LVMI) than controls (all $p < 0.0001$) and significantly lower left ventricular end-diastolic dimension (LVDd) and E/A (both $p < 0.001$) [75]. The authors concluded that LV twist analysis has good sensitivity and specificity in indicating the severity of myocardial fibrosis in HCM patients [75].

Another study utilizing standard echocardiography, 3-dimensional speckle tracking echocardiography measured peak systolic longitudinal, circumferential, and area strain, LSt, CSt, and ASt, respectively, to quantify LV systolic myocardial mechanics. LGE CMR in HCM patients revealed the area strain as a net result from longitudinal and circumferential deformations. This measurement correlated with functional parameters and the number of significantly hypertrophied segments detected on 2D echo and CMR. All three deformation parameters were attenuated in those myocardial segments with hypertrophy and LGE scar. There was no difference in strain parameters between hypertrophied and LGE segments. They thus concluded that these data demonstrate that hypertrophy seem to be the major independent factors altering global systolic myocardial mechanics in HCM.

In other conditions such as Fabrys disease (FD), it has been proven that fibrosis, as evidenced by the presence of LGE, is associated with lower longitudinal strain (as measured by speckle tracking) in the corresponding fibrotic wall segments [76]. Speckle tracking can thus be used as a tool for the indirect evaluation of LGE and thus myocardial fibrosis in FD. Its use has also been studied in conditions such as severe aortic stenosis [77], and in patients with

cardiotoxicity from prior Anthracycline use [78]. In cardiac amyloidosis (CA), speckle tracking echo reveals regional variations in longitudinal strain (LS) from base to apex [79] and with a relative 'apical sparing' pattern of LS, this allows us to differentiate CA from other causes of LV hypertrophy (Figs. 4.5 and 4.6).

In clinical practice, the widespread use of speckle tracking has not been seen to date, likely related to the increased time required for data analysis, however as a research tool it has a fundamental role to play in the evaluation of myocardial fibrosis.

Cardiac Computed Tomography (Multidetector CT)

Cardiac CT thus far has demonstrated initial utility predominantly for the evaluation of myocardial scar. Lardo et al. [80] demonstrated in an animal model that the spatial extent of acute and healed MI could be determined and quantified accurately with contrast-enhanced CT. In this study, the CT findings were compared to histology. Bettencourt et al. [81] found that CT delayed enhancement had good accuracy (90%) for ischemic scar detection with low sensitivity (53%) but
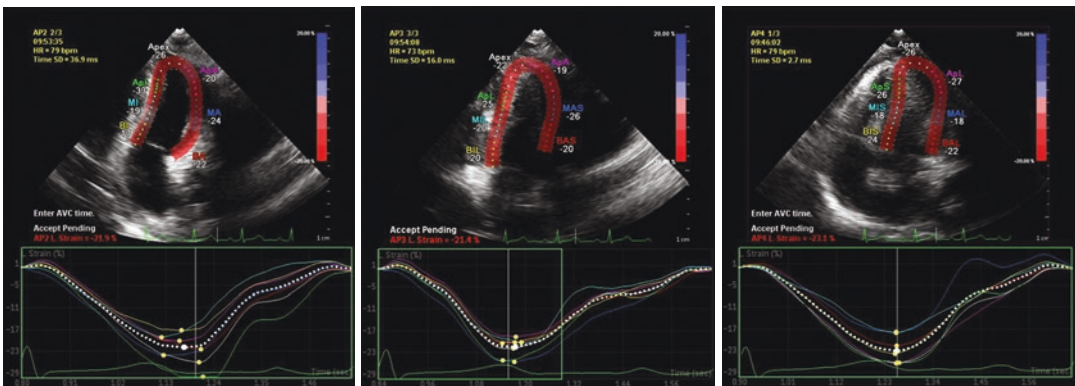
Fig. 4.5 Longitudinal Strain Measurement in a Normal Individual, measured from the 2 chamber view, 3 chamber view and 4 chamber view, respectively, in the same patient (left to right). Shortening is indicated by negative values, which range from −17 to −33, indicating regional variation in a normal heart
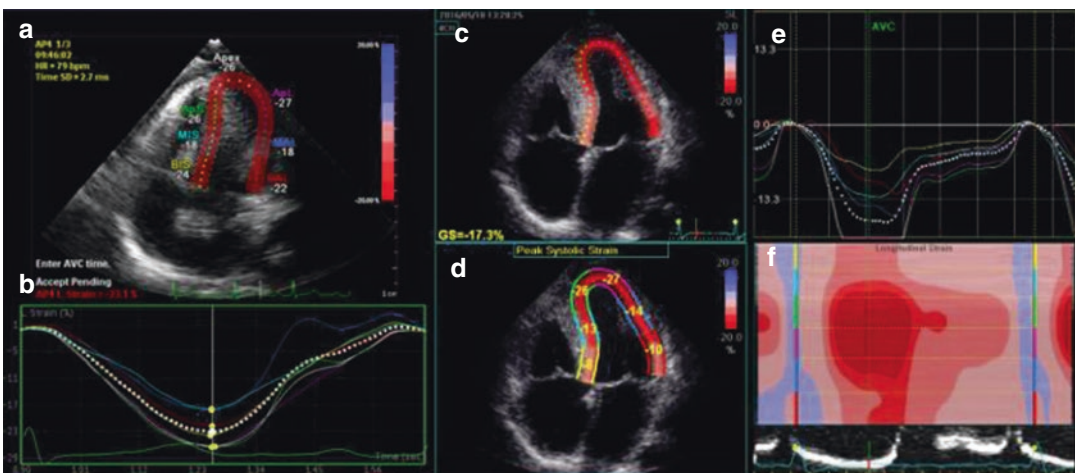
Fig. 4.6 Normal regional and global strain in a normal individual (**a**, **b**). In contrast the images from panels (**c**–**f**) are taken from a patient with cardiac amyloidosis. There is abnormal longitudinal strain affecting the basal segments with relative sparing of the apical segments and reduced overall global longitudinal strain

excellent specificity (98%). The use of MDCT for diffuse abnormalities of myocardial tissue is significantly more challenging than the evaluation of focal myocardial scar due to the low contrast resolution of CT scanning [82]. ECV measured with cardiac CT represents a novel approach toward the clinical assessment of diffuse myocardial fibrosis. It has been shown that there is a good correlation between myocardial ECV measured with cardiac CT and with T1 map measured by cardiac MR imaging in 24 subjects [83]. This study included patients with heart failure and normal controls and showed that ECV was higher in patients with heart failure for both cardiac CT and cardiac MR imaging. Also, for both cardiac MR and cardiac CT, ECV was positively associated with end diastolic and end systolic volumes and inversely related to ejection fraction (EF).

Additional supportive data for MDCT comes from Bandula et al. [84] who demonstrated that ECV measured using a equilibrium CT technique in patients with aortic stenosis correlated well with histologic quantification of myocardial fibrosis, and also with ECV derived by using equilibrium MR imaging. From a clinical perspective, MDCT has also been studied in hypertrophic cardiomyopathy [85] and found to reliably detect myocardial fibrosis as evident by LGE. Patient- and segment-based sensitivity was 100% and 68%, respectively, compared to LGE-CMR. In patients with a contraindication to CMR, this technique could therefore be useful.

Conclusion

The use of noninvasive imaging methods of myocardial fibrosis has increased in recent years. Exciting and novel techniques will continue to emerge in the years to come. Cardiac MRI has proven to be an important tool through the use of LGE-CMR and T1 mapping techniques, both in the clinical and research arena. Clinically it is now possible to carry out a full study and answer the question regarding the presence or absence of underlying myocardial fibrosis in under 45 min. In the presence of claustrophobia, non-CMR compatible devices, and inability to breath hold, alternative imaging techniques must be

considered. Echo is a reliable clinical and research tool, which has been well validated in this area. Nuclear techniques for detection of myocardial scar and myocardial viability play an important role in clinical practice. Molecular techniques are still very much research tools but are promising for future use in this field. MDCT has also proven its use as described above although the radiation dose makes it a less attractive option.

Overall, cardiac MRI has a proven benefit in the detection of underlying myocardial fibrosis. It is hoped that with earlier detection, therapies may be developed to tackle myocardial disease prior to the development of heart failure symptoms and signs.

References

1. de Haas HJ, Arbustini E, Fuster V, Kramer CM, Narula J. Molecular imaging of the cardiac extracellular matrix. Circ Res. 2014;114(5):903–15.
2. Weber KT, Janicki JS, Shroff SG, Pick R, Chen RM, Bashey RI. Collagen remodeling of the pressure-overloaded, hypertrophied nonhuman primate myocardium. Circ Res. 1988;62(4):757–65.
3. Borer JS, Truter S, Herrold EM, Falcone DJ, Pena M, Carter JN, et al. Myocardial fibrosis in chronic aortic regurgitation: molecular and cellular responses to volume overload. Circulation. 2002;105(15):1837–42.
4. Tanaka M, Fujiwara H, Onodera T, Wu DJ, Hamashima Y, Kawai C. Quantitative analysis of myocardial fibrosis in normals, hypertensive hearts, and hypertrophic cardiomyopathy. Br Heart J. 1986;55(6):575–81.
5. Tandri H, Saranathan M, Rodriguez ER, Martinez C, Bomma C, Nasir K, et al. Noninvasive detection of myocardial fibrosis in arrhythmogenic right ventricular cardiomyopathy using delayed-enhancement magnetic resonance imaging. J Am Coll Cardiol. 2005;45(1):98–103.
6. Assomull RG, Prasad SK, Lyne J, Smith G, Burman ED, Khan M, et al. Cardiovascular magnetic resonance, fibrosis, and prognosis in dilated cardiomyopathy. J Am Coll Cardiol. 2006;48(10):1977–85.
7. van den Borne SW, Isobe S, Verjans JW, Petrov A, Lovhaug D, Li P, et al. Molecular imaging of interstitial alterations in remodeling myocardium after myocardial infarction. J Am Coll Cardiol. 2008;52(24):2017–28.
8. Martos R, Baugh J, Ledwidge M, O'Loughlin C, Conlon C, Patle A, et al. Diastolic heart failure: evidence of increased myocardial collagen turnover linked to diastolic dysfunction. Circulation. 2007;115(7):888–95.

9. Mewton N, Liu CY, Croisille P, Bluemke D, Lima JA. Assessment of myocardial fibrosis with cardiovascular magnetic resonance. J Am Coll Cardiol. 2011;57(8):891–903.

10. Mahrholdt H, Goedecke C, Wagner A, Meinhardt G, Athanasiadis A, Vogelsberg H, et al. Cardiovascular magnetic resonance assessment of human myocarditis: a comparison to histology and molecular pathology. Circulation. 2004;109(10):1250–8.

11. Bocchi EA, Kalil R, Bacal F, de Lourdes Higuchi M, Meneghetti C, Magalhaes A, et al. Magnetic resonance imaging in chronic chagas' disease: correlation with endomyocardial biopsy findings and gallium-67 cardiac uptake. Echocardiography. 1998;15(3):279–88.

12. Kim RJ, Chen EL, Lima JA, Judd RM. Myocardial Gd-DTPA kinetics determine MRI contrast enhancement and reflect the extent and severity of myocardial injury after acute reperfused infarction. Circulation. 1996;94(12):3318–26.

13. Debl K, Djavidani B, Buchner S, Lipke C, Nitz W, Feuerbach S, et al. Delayed hyperenhancement in magnetic resonance imaging of left ventricular hypertrophy caused by aortic stenosis and hypertrophic cardiomyopathy: visualisation of focal fibrosis. Heart. 2006;92(10):1447–51.

14. De Cobelli F, Pieroni M, Esposito A, Chimenti C, Belloni E, Mellone R, et al. Delayed gadolinium-enhanced cardiac magnetic resonance in patients with chronic myocarditis presenting with heart failure or recurrent arrhythmias. J Am Coll Cardiol. 2006;47(8):1649–54.

15. Choudhury L, Mahrholdt H, Wagner A, Choi KM, Elliott MD, Klocke FJ, et al. Myocardial scarring in asymptomatic or mildly symptomatic patients with hypertrophic cardiomyopathy. J Am Coll Cardiol. 2002;40(12):2156–64.

16. McCrohon JA, Moon JC, Prasad SK, McKenna WJ, Lorenz CH, Coats AJ, et al. Differentiation of heart failure related to dilated cardiomyopathy and coronary artery disease using gadolinium-enhanced cardiovascular magnetic resonance. Circulation. 2003;108(1):54–9.

17. Mahrholdt H, Wagner A, Judd RM, Sechtem U, Kim RJ. Delayed enhancement cardiovascular magnetic resonance assessment of non-ischaemic cardiomyopathies. Eur Heart J. 2005;26(15):1461–74.

18. Rehwald WG, Fieno DS, Chen EL, Kim RJ, Judd RM. Myocardial magnetic resonance imaging contrast agent concentrations after reversible and irreversible ischemic injury. Circulation. 2002;105(2):224–9.

19. Croisille P, Revel D, Saeed M. Contrast agents and cardiac MR imaging of myocardial ischemia: from bench to bedside. Eur Radiol. 2006;16(9):1951–63.

20. Messroghli DR, Radjenovic A, Kozerke S, Higgins DM, Sivananthan MU, Ridgway JP. Modified look-locker inversion recovery (MOLLI) for high-resolution T1 mapping of the heart. Magn Reson Med. 2004;52(1):141–6.

21. Piechnik SK, Ferreira VM, Dall'Armellina E, Cochlin LE, Greiser A, Neubauer S, et al. Shortened modified look-locker Inversion recovery (ShMOLLI) for clinical myocardial T1-mapping at 1.5 and 3 T within a 9 heartbeat breathhold. J Cardiovasc Magn Reson. 2010;12:69.

22. Robbers LF, Baars EN, Brouwer WP, Beek AM, Hofman MB, Niessen HW, et al. T1 mapping shows increased extracellular matrix size in the myocardium due to amyloid depositions. Circ Cardiovasc Imaging. 2012;5(3):423–6.

23. Iles L, Pfluger H, Phrommintikul A, Cherayath J, Aksit P, Gupta SN, et al. Evaluation of diffuse myocardial fibrosis in heart failure with cardiac magnetic resonance contrast-enhanced T1 mapping. J Am Coll Cardiol. 2008;52(19):1574–80.

24. Sibley CT, Noureldin RA, Gai N, Nacif MS, Liu S, Turkbey EB, et al. T1 mapping in cardiomyopathy at cardiac MR: comparison with endomyocardial biopsy. Radiology. 2012;265(3):724–32.

25. Messroghli DR, Niendorf T, Schulz-Menger J, Dietz R, Friedrich MG. T1 mapping in patients with acute myocardial infarction. J Cardiovasc Magn Reson. 2003;5(2):353–9.

26. Maceira AM, Joshi J, Prasad SK, Moon JC, Perugini E, Harding I, et al. Cardiovascular magnetic resonance in cardiac amyloidosis. Circulation. 2005;111(2):186–93.

27. Messroghli DR, Walters K, Plein S, Sparrow P, Friedrich MG, Ridgway JP, et al. Myocardial T1 mapping: application to patients with acute and chronic myocardial infarction. Magn Reson Med. 2007;58(1):34–40.

28. Broberg CS, Chugh SS, Conklin C, Sahn DJ, Jerosch-Herold M. Quantification of diffuse myocardial fibrosis and its association with myocardial dysfunction in congenital heart disease. Circ Cardiovasc Imaging. 2010;3(6):727–34.

29. Flett AS, Hayward MP, Ashworth MT, Hansen MS, Taylor AM, Elliott PM, et al. Equilibrium contrast cardiovascular magnetic resonance for the measurement of diffuse myocardial fibrosis: preliminary validation in humans. Circulation. 2010;122(2):138–44.

30. Gai N, Turkbey EB, Nazarian S, van der Geest RJ, Liu CY, Lima JA, et al. T1 mapping of the gadolinium-enhanced myocardium: adjustment for factors affecting interpatient comparison. Magn Reson Med. 2011;65(5):1407–15.

31. Bauner KU, Biffar A, Theisen D, Greiser A, Zech CJ, Nguyen ET, et al. Extracellular volume fractions in chronic myocardial infarction. Investig Radiol. 2012;47(9):538–45.

32. Turkbey EB, Gai N, Lima JA, van der Geest RJ, Wagner KR, Tomaselli GF, et al. Assessment of cardiac involvement in myotonic muscular dystrophy by T1 mapping on magnetic resonance imaging. Heart Rhythm. 2012;9(10):1691–7.

33. Dass S, Suttie JJ, Piechnik SK, Ferreira VM, Holloway CJ, Banerjee R, et al. Myocardial tissue characterization using magnetic resonance noncontrast t1 mapping in hypertrophic and dilated cardiomyopathy. Circ Cardiovasc Imaging. 2012;5(6):726–33.

34. Fontana M, White SK, Banypersad SM, Sado DM, Maestrini V, Flett AS, et al. Comparison of T1 mapping techniques for ECV quantification. Histological validation and reproducibility of ShMOLLI versus multibreath-hold T1 quantification equilibrium contrast CMR. J Cardiovasc Magn Reson. 2012;14:88.

35. Rao AD, Shah RV, Garg R, Abbasi SA, Neilan TG, Perlstein TS, et al. Aldosterone and myocardial extracellular matrix expansion in type 2 diabetes mellitus. Am J Cardiol. 2013;112(1):73–8.

36. Ellims AH, Shaw JA, Stub D, Iles LM, Hare JL, Slavin GS, et al. Diffuse myocardial fibrosis evaluated by post-contrast t1 mapping correlates with left ventricular stiffness. J Am Coll Cardiol. 2014;63(11):1112–8.

37. Schulz-Menger J, Bluemke DA, Bremerich J, Flamm SD, Fogel MA, Friedrich MG, et al. Standardized image interpretation and post processing in cardiovascular magnetic resonance: Society for Cardiovascular Magnetic Resonance (SCMR) board of trustees task force on standardized post processing. J Cardiovasc Magn Reson. 2013;15:35.

38. Gatehouse PD, Bydder GM. Magnetic resonance imaging of short T2 components in tissue. Clin Radiol. 2003;58(1):1–19.

39. de Jong S, Zwanenburg JJ, Visser F, der Nagel R, van Rijen HV, Vos MA, et al. Direct detection of myocardial fibrosis by MRI. J Mol Cell Cardiol. 2011;51(6):974–9.

40. Siu AG, Ramadeen A, Hu X, Morikawa L, Zhang L, Lau JY, et al. Characterization of the ultrashort-TE (UTE) MR collagen signal. NMR Biomed. 2015;28(10):1236–44.

41. Vandsburger M, Vandoorne K, Oren R, Leftin A, Mpofu S, Delli Castelli D, et al. Cardio-chemical exchange saturation transfer magnetic resonance imaging reveals molecular signatures of endogenous fibrosis and exogenous contrast media. Circ Cardiovasc Imaging. 2015;8(1).

42. Helm PA, Caravan P, French BA, Jacques V, Shen L, Xu Y, et al. Postinfarction myocardial scarring in mice: molecular MR imaging with use of a collagen-targeting contrast agent. Radiology. 2008;247(3):788–96.

43. Jellis C, Martin J, Narula J, Marwick TH. Assessment of nonischemic myocardial fibrosis. J Am Coll Cardiol. 2010;56(2):89–97.

44. Yamamoto Y, de Silva R, Rhodes CG, Araujo LI, Iida H, Rechavia E, et al. A new strategy for the assessment of viable myocardium and regional myocardial blood flow using 15O-water and dynamic positron emission tomography. Circulation. 1992;86(1):167–78.

45. Knaapen P, Boellaard R, Gotte MJ, Dijkmans PA, van Campen LM, de Cock CC, et al. Perfusable tissue index as a potential marker of fibrosis in patients with idiopathic dilated cardiomyopathy. J Nucl Med. 2004;45(8):1299–304.

46. Knaapen P, Gotte MJ, Paulus WJ, Zwanenburg JJ, Dijkmans PA, Boellaard R, et al. Does myocardial fibrosis hinder contractile function and perfusion in idiopathic dilated cardiomyopathy? PET and MR imaging study. Radiology. 2006;240(2):380–8.

47. Knaapen P, van Dockum WG, Bondarenko O, Kok WE, Gotte MJ, Boellaard R, et al. Delayed contrast enhancement and perfusable tissue index in hypertrophic cardiomyopathy: comparison between cardiac MRI and PET. J Nucl Med. 2005;46(6):923–9.

48. van den Borne SW, Isobe S, Zandbergen HR, Li P, Petrov A, Wong ND, et al. Molecular imaging for efficacy of pharmacologic intervention in myocardial remodeling. JACC Cardiovasc Imaging. 2009;2(2):187–98.

49. Tadamura E, Kudoh T, Hattori N, Inubushi M, Magata Y, Konishi J, et al. Impairment of BMIPP uptake precedes abnormalities in oxygen and glucose metabolism in hypertrophic cardiomyopathy. J Nucl Med. 1998;39(3):390–6.

50. Delgado V, Bax JJ. Clinical topic: Nuclear imaging in hypertrophic cardiomyopathy. J Nucl Cardiol. 2015;22(3):408–18.

51. Hashimura H, Kiso K, Yamada N, Kono A, Morita Y, Fukushima K, et al. Myocardial impairment detected by late gadolinium enhancement in hypertrophic cardiomyopathy: comparison with 99mTc-MIBI/tetrofosmin and 123I-BMIPP SPECT. Kobe J Med Sci. 2013;59(3):E81–92.

52. Mimbs JW, O'Donnell M, Bauwens D, Miller JW, Sobel BE. The dependence of ultrasonic attenuation and backscatter on collagen content in dog and rabbit hearts. Circ Res. 1980;47(1):49–58.

53. Shapiro LM, Moore RB, Logan-Sinclair RB, Gibson DG. Relation of regional echo amplitude to left ventricular function and the electrocardiogram in left ventricular hypertrophy. Br Heart J. 1984;52(1):99–105.

54. Picano E, Pelosi G, Marzilli M, Lattanzi F, Benassi A, Landini L, et al. In vivo quantitative ultrasonic evaluation of myocardial fibrosis in humans. Circulation. 1990;81(1):58–64.

55. Lin YH, Shiau YC, Yen RF, Lin LC, Wu CC, Ho YL, et al. The relation between myocardial cyclic variation of integrated backscatter and serum concentrations of procollagen propeptides in hypertensive patients. Ultrasound Med Biol. 2004;30(7):885–91.

56. Naito J, Masuyama T, Mano T, Kondo H, Yamamoto K, Nagano R, et al. Analysis of transmural trend of myocardial integrated ultrasonic backscatter in patients with old myocardial infarction. Ultrasound Med Biol. 1996;22(7):807–14.

57. Fang ZY, Leano R, Marwick TH. Relationship between longitudinal and radial contractility in subclinical diabetic heart disease. Clin Sci (Lond). 2004;106(1):53–60.

58. Mele D, Censi S, La Corte R, Merli E, Lo Monaco A, Locaputo A, et al. Abnormalities of left ventricular function in asymptomatic patients with systemic sclerosis using Doppler measures of myocardial strain. J Am Soc Echocardiogr. 2008;21(11):1257–64.

59. Ho CY, Solomon SD. A clinician's guide to tissue Doppler imaging. Circulation. 2006;113(10):e396–8.

60. Vinereanu D, Khokhar A, Fraser AG. Reproducibility of pulsed wave tissue Doppler echocardiography. J Am Soc Echocardiogr. 1999;12(6):492–9.

61. Galiuto L, Ignone G, DeMaria AN. Contraction and relaxation velocities of the normal left ventricle using

pulsed-wave tissue Doppler echocardiography. Am J Cardiol. 1998;81(5):609–14.

62. Yamada H, Oki T, Mishiro Y, Tabata T, Abe M, Onose Y, et al. Effect of aging on diastolic left ventricular myocardial velocities measured by pulsed tissue Doppler imaging in healthy subjects. J Am Soc Echocardiogr. 1999;12(7):574–81.

63. Fang ZY, Schull-Meade R, Downey M, Prins J, Marwick TH. Determinants of subclinical diabetic heart disease. Diabetologia. 2005;48(2):394–402.

64. Shan K, Bick RJ, Poindexter BJ, Shimoni S, Letsou GV, Reardon MJ, et al. Relation of tissue Doppler derived myocardial velocities to myocardial structure and beta-adrenergic receptor density in humans. J Am Coll Cardiol. 2000;36(3):891–6.

65. Park J, Chang HJ, Choi JH, Yang PS, Lee SE, Heo R, et al. Late gadolinium enhancement in cardiac MRI in patients with severe aortic stenosis and preserved left ventricular systolic function is related to attenuated improvement of left ventricular geometry and filling pressure after aortic valve replacement. Korean Circ J. 2014;44(5):312–9.

66. Moreo A, Ambrosio G, De Chiara B, Pu M, Tran T, Mauri F, et al. Influence of myocardial fibrosis on left ventricular diastolic function: noninvasive assessment by cardiac magnetic resonance and echo. Circ Cardiovasc Imaging. 2009;2(6):437–43.

67. Shah AM, Solomon SD. Myocardial deformation imaging: current status and future directions. Circulation. 2012;125(2):e244–8.

68. Oh JK, James Seward JB, Tajik AJ. The echo manual. 3rd ed. Philadelphia: Lippincott Williams & Wilkins; 2007.

69. Helle-Valle T, Crosby J, Edvardsen T, Lyseggen E, Amundsen BH, Smith HJ, et al. New noninvasive method for assessment of left ventricular rotation: speckle tracking echocardiography. Circulation. 2005;112(20):3149–56.

70. Masci PG, Marinelli M, Piacenti M, Lorenzoni V, Positano V, Lombardi M, et al. Myocardial structural, perfusion, and metabolic correlates of left bundle branch block mechanical derangement in patients with dilated cardiomyopathy: a tagged cardiac magnetic resonance and positron emission tomography study. Circ Cardiovasc Imaging. 2010;3(4):482–90.

71. Nahum J, Bensaid A, Dussault C, Macron L, Clemence D, Bouhemad B, et al. Impact of longitudinal myocardial deformation on the prognosis of chronic heart failure patients. Circ Cardiovasc Imaging. 2010;3(3):249–56.

72. Hung CL, Verma A, Uno H, Shin SH, Bourgoun M, Hassanein AH, et al. Longitudinal and circumferential strain rate, left ventricular remodeling, and prognosis after myocardial infarction. J Am Coll Cardiol. 2010;56(22):1812–22.

73. Cho GY, Marwick TH, Kim HS, Kim MK, Hong KS, Oh DJ. Global 2-dimensional strain as a new prognosticator in patients with heart failure. J Am Coll Cardiol. 2009;54(7):618–24.

74. Sengupta PP, Khandheria BK, Korinek J, Wang J, Jahangir A, Seward JB, et al. Apex-to-base dispersion in regional timing of left ventricular shortening and lengthening. J Am Coll Cardiol. 2006;47(1):163–72.

75. Zhang HJ, Wang H, Sun T, Lu MJ, Xu N, Wu WC, et al. Assessment of left ventricular twist mechanics by speckle tracking echocardiography reveals association between LV twist and myocardial fibrosis in patients with hypertrophic cardiomyopathy. Int J Cardiovasc Imaging. 2014;30(8):1539–48.

76. Kramer J, Niemann M, Liu D, Hu K, Machann W, Beer M, et al. Two-dimensional speckle tracking as a non-invasive tool for identification of myocardial fibrosis in Fabry disease. Eur Heart J. 2013;34(21):1587–96.

77. Hoffmann R, Altiok E, Friedman Z, Becker M, Frick M. Myocardial deformation imaging by two-dimensional speckle-tracking echocardiography in comparison to late gadolinium enhancement cardiac magnetic resonance for analysis of myocardial fibrosis in severe aortic stenosis. Am J Cardiol. 2014;114(7):1083–8.

78. Ho E, Brown A, Barrett P, Morgan RB, King G, Kennedy MJ, et al. Subclinical anthracycline- and trastuzumab-induced cardiotoxicity in the long-term follow-up of asymptomatic breast cancer survivors: a speckle tracking echocardiographic study. Heart. 2010;96(9):701–7.

79. Phelan D, Collier P, Thavendiranathan P, Popovic ZB, Hanna M, Plana JC, et al. Relative apical sparing of longitudinal strain using two-dimensional speckle-tracking echocardiography is both sensitive and specific for the diagnosis of cardiac amyloidosis. Heart. 2012;98(19):1442–8.

80. Lardo AC, Cordeiro MA, Silva C, Amado LC, George RT, Saliaris AP, et al. Contrast-enhanced multidetector computed tomography viability imaging after myocardial infarction: characterization of myocyte death, microvascular obstruction, and chronic scar. Circulation. 2006;113(3):394–404.

81. Bettencourt N, Rocha J, Carvalho M, Leite D, Toschke AM, Melica B, et al. Multislice computed tomography in the exclusion of coronary artery disease in patients with presurgical valve disease. Circ Cardiovasc Imaging. 2009;2(4):306–13.

82. Pattanayak P, Bleumke DA. Tissue characterization of the myocardium: state of the art characterization by magnetic resonance and computed tomography imaging. Radiol Clin N Am. 2015;53(2):413–23.

83. Nacif MS, Kawel N, Lee JJ, Chen X, Yao J, Zavodni A, et al. Interstitial myocardial fibrosis assessed as extracellular volume fraction with low-radiation-dose cardiac CT. Radiology. 2012;264(3):876–83.

84. Bandula S, White SK, Flett AS, Lawrence D, Pugliese F, Ashworth MT, et al. Measurement of myocardial extracellular volume fraction by using equilibrium contrast-enhanced CT: validation against histologic findings. Radiology. 2013;269(2):396–403.

85. Langer C, Lutz M, Eden M, Ludde M, Hohnhorst M, Gierloff C, et al. Hypertrophic cardiomyopathy in cardiac CT: a validation study on the detection of intramyocardial fibrosis in consecutive patients. Int J Cardiovasc Imaging. 2014;30(3):659–67.